Spatially resolved refractive index profiles of electrically switchable computer-generated holographic gratings

Gianluigi Zito, Andrea Finizio, and Sergio De Nicola*

Istituto di Cibernetica "E. Caianiello" del Consiglio Nazionale delle Ricerche, Via Campi Flegrei 34, 80078 Pozzuoli (Na), Italy
**s.denicola@cib.na.cnr.it*

Abstract: We describe a spatially resolved interferometric technique combined with a phase reconstruction method that provides a quantitative two-dimensional profile of the refractive index and spatial distribution of the optical contrast between the on-off states of electrically switchable diffraction gratings as a function of the external electric field. The studied structures are holographic gratings optically written into polymer/liquid crystal composites through single-beam spatial light modulation by means of computer-generated holograms. The electro-optical response of the gratings is also discussed. The diffraction efficiency results to be dependent on the incident light polarization suggesting the possibility to develop polarization dependent switching devices.

OCIS codes: (090.1760) Computer holography; (230.6120) Spatial light modulators; (090.2880) Holographic Interferometry.

References and links

1. T. K. Gaylord, and M. G. Moharam, "Analysis and application of optical diffraction by gratings," *in Proceedings of IEEE* **73,** 894–937 (1985).
2. L. Eldada, "Optical communication components," Rev. Sci. Instrum. **75**(3), 575–593 (2004).
3. R. L. Sutherland, V. P. Tondiglia, L. V. Natarajan, T. J. Bunning, and W. W. Adams, L. V. Natarajan V. P. Tondiglia, T. J. Bunning, and W. W. Adams, "Electrically switchable volume gratings in polymer-dispersed liquid crystals," Appl. Phys. Lett. **64**(9), 1074 (1994).
4. R. L. Sutherland, L. V. Natarajan, V. P. Tondiglia, and T. J. Bunning, "Bragg gratings in an acrylate polymer consisting of periodic polymer-dispersed liquid-crystal planes," Chem. Mater. **5**(10), 1533–1538 (1993).
5. D. H. Close, A. D. Jacobson, J. D. Margerum, R. G. Brault, and F. J. Mc Clung, "Hologram recorded on photopolymer holographic recording material," Appl. Phys. Lett. **14**, 159–160 (1969).
6. R. Asquini, A. D'Alessandro, C. Gizzi, P. Maltese, R. Caputo, A. V. Sukhov, C. Umeton, and A. Veltri, "Optical characterization at wavelengths of 632.8 nm and 1549 nm of POLICRYPS switchable diffraction gratings," Mol. Cryst. Liq. Cryst. (Phila. Pa.) **398**(1), 223–233 (2003).
7. G. Zito, B. Piccirillo, E. Santamato, A. Marino, V. Tkachenko, and G. Abbate, "Computer-generated holographic gratings in soft matter," Mol. Cryst. Liq. Cryst. (Phila. Pa.) **465**(1), 371–378 (2007).
8. G. Zito, B. Piccirillo, E. Santamato, A. Marino, V. Tkachenko, and G. Abbate, "Two-dimensional photonic quasicrystals by single beam computer-generated holography," Opt. Express **16**(8), 5164–5170 (2008).
9. V. A. Soifer, ed., *Methods for Computer Design of Diffractive Optical Elements* (John Wiley & Sons, Inc., New York, 2002).
10. F. Vita, A. Marino, V. Tkachenko, G. Abbate, D. E. Lucchetta, L. Criante, and F. Simoni, "Visible and near-infrared characterization and modeling of nanosized holographic-polymer-dispersed liquid crystal gratings," Phys. Rev. E Stat. Nonlin. Soft Matter Phys. **72**(1), 011702 (2005).
11. F. Simoni, *Nonlinear Optical Properties of Liquid Crystals and Polymer Dispersed Liquid Crystals* (World Scientific, Singapore, 1997).
12. M. de Angelis, S. De Nicola, A. Finizio, G. Pierattini, P. Ferraro, S. Pelli, G. Righini, and S. Sebastiani, "Digital-holography refractive-index-profile measurement of phase gratings," Appl. Phys. Lett. **88**(11), 111114 (2006).
13. P. Hariharan, *Basics of Holography* (Cambridge University Press, New York, 2002), Chap. 13.
14. C. L. Curl, C. J. Bellair, T. Harris, B. E. Allman, P. J. Harris, A. G. Stewart, A. Roberts, K. A. Nugent, and L. M. D. Delbridge, B.E. Allman, O. J. Harris, A.G. Stewart, A. Roberts, K.A. Nugebt and L. M. D. Delbridge, "Refractive index measurement in viable cells using quantitative phase-amplitude microscopy and confocal microscopy," Cytometry **65A**(1), 88–92 (2005).

#115297 - $15.00 USD Received 4 Aug 2009; revised 24 Sep 2009; accepted 28 Sep 2009; published 2 Oct 2009

15. B. Rappaz, F. Charrière, C. Depeursinge, P. J. Magistretti, and P. Marquet, "Simultaneous cell morphometry and refractive index measurement with dual-wavelength digital holographic microscopy and dye-enhanced dispersion of perfusion medium," Opt. Lett. **33**(7), 744–746 (2008).
16. T. Colomb, F. Dürr, E. Cuche, P. Marquet, H. G. Limberger, R. P. Salathé, and C. Depeursinge, "Polarization microscopy by use of digital holography: application to optical-fiber birefringence measurements," Appl. Opt. **44**(21), 4461–4469 (2005).
17. M. Y. Yokota, Y. Terui, and I. Yamaguchi, "Polarization analysis with digital holography by use of polarization modulation for single reference beam," Opt. Eng. **46**(5), 055801–055807 (2007).
18. C. Meneses-Fabian, G. Rodriguez-Zurita, M.-C. Encarnacion-Gutierrez, and N. I. Toto-Arellano, M. –del- C. Encarnacion-Gutierrez, N. I. Toto-Arellano, "Phase-shifting interferometry with four interferograms using linear polarization modulation and a Ronchi grating displaced by only a small unknown amount," Opt. Commun. **282**(15), 3063–3068 (2009).
19. J. W. Goodman, ed., *Introduction to Fourier Optics* (McGraw-Hill, New York, 1996).

1. Introduction

Diffraction of optical electromagnetic radiation by periodic structures like Bragg gratings is of increasing importance in an expanding variety of engineering applications in the fields of photonics, acousto-optics, integrated optics, holography, optical data processing and spectral analysis [1,2]. The use of liquid crystals (LCs), in composites with polymers or infiltrated in patterned materials for realizing diffraction gratings or more complex functionalized structures allows electrical control of the realized devices [3]. These materials exhibit very attracting optical, mechanical, chemical and thermal properties and flexible processing techniques. Combined with fabrication techniques like two-beam holography [4], they can be patterned quite easily into several unique structures, in which the record of the holographic interference pattern usually takes the form of a sinusoidal spatial modulation of the absorption constant or the refractive index of the medium, or both. Photopolymer materials yield modulations of the refractive index [5]. Two-beam holography has been largely used to produce gratings in polymer-liquid crystal composites, like holographic polymer-dispersed liquid crystal (H-PDLC) gratings [3,4] and polymer-liquid crystal-polymer slice (POLICRYPS) structures [6].

The microscopic structure of polymer-LC based Bragg gratings is affected by the LC-polymer phase separation, as well as by the optical anisotropy of the LC-droplet director, the mixture composition, the geometrical parameters, the optical curing parameters (light intensity, exposure time, sample temperature). Great efforts have been dedicated to acquire a full comprehension of the microscopic structure of soft matter diffraction gratings, as for instance nuclear magnetic resonance, scanning electron and atomic force microscopy, and optical and electro-optical characterizations.

Recently, a different single-beam holographic technique, based on the spatial light modulation of the writing light irradiance by means of computer-generated holograms (CGHs) encoded into a programmable spatial light modulator (SLM), has been employed in the production of soft material diffraction gratings [7], and even of more complex photonic structures, like aperiodic or quasiperiodic ones [8]. The CGH is addressed to the liquid crystal display of the SLM which acts as a diffractive optical element (DOE) [9]. Almost any desired dielectric structure can be optically designed by impinging the generated pattern onto photosensitive materials.

In this work, we present a spatially resolved interferometric technique combined with a phase reconstruction method that provides an electro-optic characterization of CGH diffraction gratings optically recorded into liquid crystal-polymer photosensitive mixtures by single-beam spatial light modulation. Off-axis digital holography is used to investigate the dielectric modulation of CGH-gratings through the quantitative determination of the dependence of the optical contrast on the applied electric field. The spatial modulation of the phase grating is then used to determine the two-dimensional spatial distribution of the refractive index profile between the ON-OFF states of the electrically switchable grating

The paper is organized as follows: in Sec. 2 the experimental electro-optical characterization of the CGH grating, i.e. the angular diffraction efficiency and the efficiency modulation as a function of the external electric field at the Bragg angle is presented and

#115297 - $15.00 USD Received 4 Aug 2009; revised 24 Sep 2009; accepted 28 Sep 2009; published 2 Oct 2009

discussed; in Sec. 3 the interferometric technique used to measure the index profile of the sample is described; in Sec. 4 the interferometric experimental results are discussed; finally in Sec. 5 our conclusions are presented.

2. Electro-optical characterization of the CGH grating

As discussed in [7,8] computer-generated holograms have been exploited in combination with a programmable spatial light modulator to produce a periodic modulation along the transverse irradiance profile of a single laser beam. The 1D periodic modulation was optically recorded into photosensitive composites consisting of a suitable prepolymer-liquid crystal mixture. The CGH gratings were produced as transmission volume phase gratings in Bragg regime with a spacing or grating path of the order of Λ=1-5μm. The analysis of the CGH gratings by a polarizing microscope revealed a good phase separation between the liquid crystal and the polymer stripes in the pattern. An average preferential alignment of the LC molecules with the molecular director along the direction normal to polymer fringe was observed. The amount of diffraction efficiency depends on the optical contrast achieved in the grating which is related to the amount of established phase separation. The application of an external electric field of amplitude E_{ext} (typically an ac square wave profile at sufficiently high frequency, say 1KHz) modulates the diffraction efficiency of the grating by reorienting the LC molecules so that the refractive index contrast between the polymer and the LC stripes is strongly reduced (ideally to zero) when almost all LC molecules are aligned with the applied external

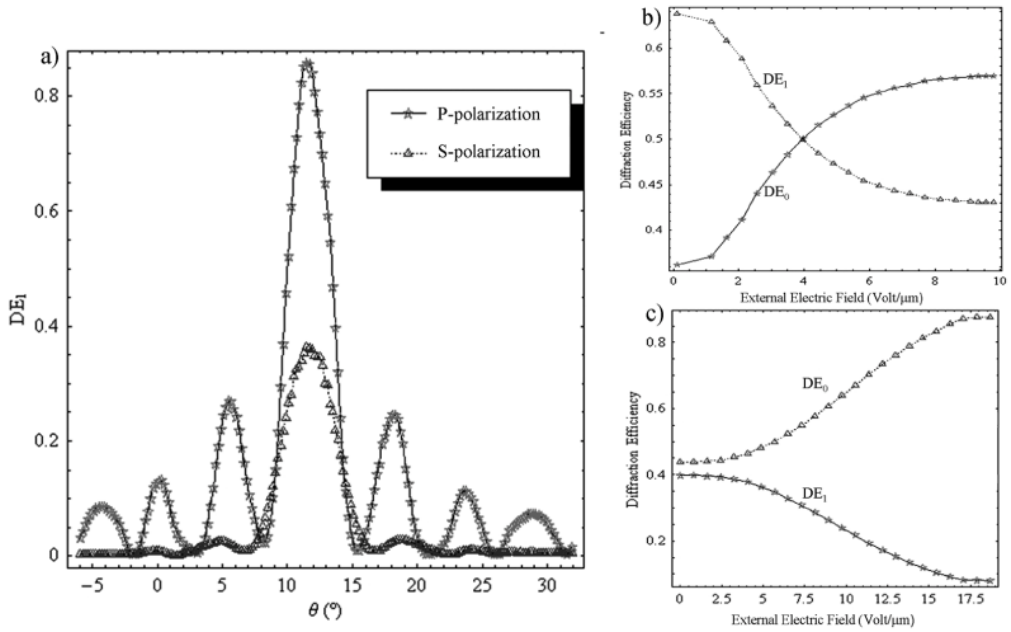

Fig. 1. Example of electro-optical characterization of the CGH diffraction gratings: (a) angular dependence of the first order diffraction efficiency DE_1 for *p*- and *s*-polarization of the incident beam on a sample of thickness d=34.3μm for wavelength 633 nm; normalized first order (DE_1) and zero order (DE_0) diffraction efficiencies, for *p*-polarization (b) and *s*-polarization (c) vs applied electric field.

field [3,6]. The electric field is applied along the direction normal to the conductive plates of the sample, coated with indium tin oxide (ITO). If our grating operates in a typical Bragg diffraction regime in the ON state, i.e. with the external electric field E_{ext}=0, most of the light is diffracted into the first order with negligible amount of light diffracted in higher orders. In Bragg diffraction regime, with the grating state OFF, i.e. with the external electric field E_{ext}=0, most the diffracted light is transmitted into the zero diffraction order.

#115297 - $15.00 USD Received 4 Aug 2009; revised 24 Sep 2009; accepted 28 Sep 2009; published 2 Oct 2009

Electro-optical characterization of the CGH-diffraction gratings was performed by measuring the angular diffraction efficiency for both *s*- and *p*-polarization, i.e. for polarization orthogonal and parallel to the plane of incidence(defined by the wave vector of the incident beam and the normal to sample plates), respectively. In Fig. 1-(a), an example of the typical angular diffraction efficiency at the first diffraction order DE_1, for *s*- and *p*-polarization, measured on CGH-gratings is shown. Diffraction efficiencies are defined as the ratio between the diffracted beam intensity and the sum of the diffracted and transmitted light intensities. Measurement the diffraction efficiency dependence on the incidence angle have been made with a He-Ne laser at the wavelength $\lambda=633nm$ by detecting the diffracted and transmitted light simultaneously as a function of the external incidence angle. The sample temperature was held constant at $T=25.0\pm0.1°C$. Experimental value of the Bragg angle ($\theta_B=11.5°$) corresponds to a grating spacing $\Lambda=1.6\mu m$ (Fig. 1-(a)). Diffraction efficiency at the Bragg angle was typically higher than 70% for *p*-polarization and lower than 45% for *s*-polarization (85% and 37%, respectively, in Fig. 1-(a)). The experimentally observed angular dependence of the CGH-diffraction grating efficiency reveals a large optically induced contrast. The diffraction efficiency measured for *p*-polarization is clearly different from the *s*-polarization, the latter being lower at the corresponding Bragg peak of about 40%.

The dependence of the diffraction efficiency on the polarization of the incident light is a clear indication of the anisotropic nature of the CGH gratings, that can be traced to a preferred alignment of the LC molecules along the grating vector [10].

The electro-optic response of the CGH gratings is determined by measuring the diffraction efficiency dependence at Bragg angle on the applied external electric field. Experimental results are shown in Fig. 1-(b) and 1-(c) for *p*- and *s*-polarization, respectively. The modulation of first diffraction order DE_1 and zero diffraction order DE_0 (transmitted light) as a function of the applied electric field E_{ext} indicates a reorientation of the LC-domains that decreases the optical contrast, leading to the switching off of the grating.

The *p*-polarization and *s*-polarization diffraction efficiencies are reduced of about 20% (Fig. 1-(b)) and 35% (Fig. 1-(c)), respectively. Switching occurs for values typically observed in the case of LC droplets in H-PDLC gratings. Therefore, it is expected that the result of the recording process of CGH gratings consist of periodic distribution of LC droplets characterized by a preferential alignment of the LC molecules. In view of their polarization and switching properties the CGH diffraction gratings can be proposed as active element for optoelectronic applications.

Quantitative indication about the CGH grating morphology can be obtained by measuring the dependence of dielectric modulation on the applied electric field. The spatially resolved interferometric technique is especially useful to infer important information about the degree of phase separation [11] and the electro-optical dependence of the anisotropy

3. Spatially resolved refractive index profiles of CGH gratings: description of the method

We perform two-dimensional visualization and optical analysis of the refractive index profile of CGH gratings by using digital holographic microscopy (DH) [12–18]. Quantitative measurement of the electrically induced birefringence or optical contrast between the ON-OFF states of the CGH grating is obtained. This provides information on the morphology, homogeneity and overall quality of the structure and allows comparison of different switching devices or simply diffractive elements for specific applications. According to the DH technique the object beam passing through the sample is superimposed to a reference beam. The phase front deformation of the object beam is a replication of the electrically modulated refractive index integrated along the CGH diffraction thickness *d*. The hologram resulting from the interference between the reference and the object fields is digitally recorded by a CCD camera. Then the wave field at the plane of the sample under test is numerically reconstructed for each value of the external voltage applied to the grating cell.

Figure 2 shows a schematic representation of the diagnostic interferometric setup is. The interferometric setup is based on a Mach-Zehnder configuration. A laser source (Coherent

#115297 - $15.00 USD Received 4 Aug 2009; revised 24 Sep 2009; accepted 28 Sep 2009; published 2 Oct 2009

Verdi) operating at wavelength λ=532nm is split into two beams at the polarized beam splitter position (PBS) in Fig. 2, the object and the reference beam impinging on the mirrors indicated as $M_{1,2}$,

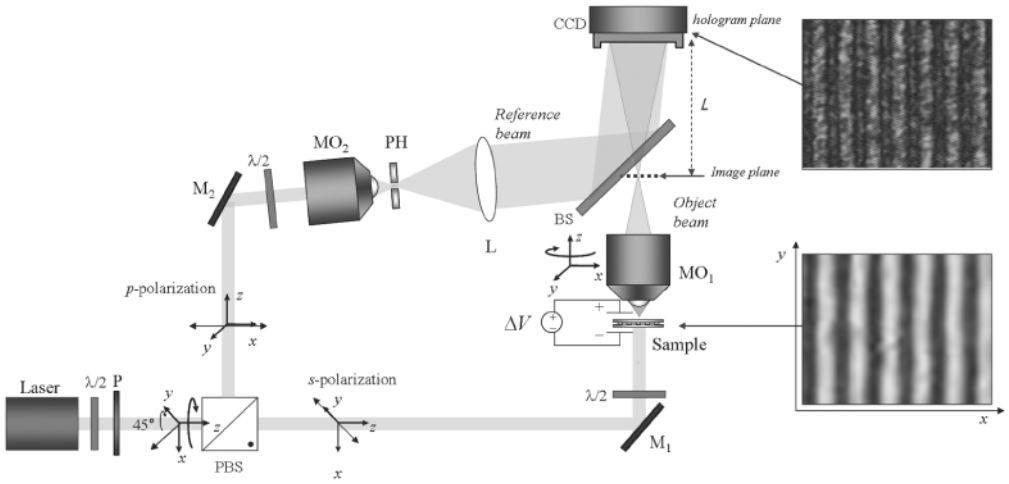

Fig. 2. Schematic representation of the interferometric holography setup used to measure the 2D spatially resolved phase profile of CGH-gratings.

respectively. A λ/2 wave-plate is inserted between the laser source and the PBS to linearly polarize the laser beam at 45° with respect to the vertical direction (y-axis). A polarizer P allows to optimize the fringe visibility and dynamical range of the digital holograms by changing the intensity of the output laser beam. After the PBS the object beam is linearly polarized along the y-direction and the reference beam is linearly polarized along the horizontal x-direction. Two additional λ/2 wave-plates are inserted after the mirrors M_1 and M_2, respectively, in order to independently control and change the orientation of the linear polarization of the object and reference beams, so that both interfering beams have the same polarization during each recording of the interference pattern. Two different measurements of the birefringent sample are performed: one for s- polarization of the interfering beams and one for p-polarization. The grating sample is inserted into the object arm of the interferometer. An image of a grating taken under a polarized microscope is shown in Fig. 2. A variable voltage ΔV is applied to the CGH sample cell of thickness d=25μm. A 20× microscope objective MO_1 is placed after the sample to allow magnification of the grating structure in the image plane and increasing the achievable spatial resolution. The reference beam, after having been spatially filtered through the microscope objective MO_2 combined with the pinhole PH, is collimated by the lens L and projected through the beam splitter BS into the CCD camera plane where it interferes with the object beam. The holograms are recorded by the CCD sensor (hologram plane) and have a resolution of $N \times N$ =1024×1024 square pixels of size $\Delta x' = \Delta y' = 6.7\mu m$. An example of interference pattern recorded at the hologram plane of coordinates is shown in Fig. 2. The complex object field $O(x, y)=A(x, y)exp[i\Phi(x, y)]$ is reconstructed at the image (x, y)-plane at a distance L=100mm from the CCD plane by using the well known Fresnel approximation [19] of the Rayleigh-Sommerfeld diffraction formula

$$O(x,y) \propto \iint H(x',y')R(x',y')exp[i\frac{\pi}{\lambda L}(x'^2+y'^2)]exp[-2i\frac{\pi}{\lambda L}(xx'+yy')]\mathrm{d}x'\mathrm{d}y', \quad (1)$$

where $R(x', y')$ is the plane wave reference, $H(x', y')$ represents the experimental hologram profile, L is the reconstruction distance. Discretization of Eq. (1) into the hologram plane and use of the sampling theorem [19] gives the resolution of the reconstructed field in the image

#115297 - $15.00 USD Received 4 Aug 2009; revised 24 Sep 2009; accepted 28 Sep 2009; published 2 Oct 2009

plane, i.e. the size of the reconstruction pixel $\Delta x = \Delta y = \lambda L / N\Delta x' \simeq 15.5\mu m$. The actual resolution achievable depends on the lateral magnification and on the numerical aperture of the microscope objective.

The numerical reconstruction of the wave field at the plane of the sample under test eliminates spreading diffraction effects because both the amplitude and phase of the object beam are reconstructed at the correct focusing distance. From the complex values of the reconstructed wave field $O||x, y|$, the intensity distribution $I(x, y)$ and the phase $\Phi(x, y)$ of the object beam can be calculated at the image plane at distance L according to the following simple relations

$$\begin{cases} I(x, y; L) = \left|O(x, y)\right|^2, \\ \Phi\left(x, y; L\right) = Arg\left\{\dfrac{\Im\left[O(x, y)\right]}{\Re\left[O(x, y)\right]}.\right\} \end{cases} \tag{2}$$

In the experiment we performed a double-exposure digital holographic interferometry. A linear voltage ramp is applied across the sample while a set of 269 digital holograms are sequentially recorded at a rate of 1 frame/*s*. The initial hologram $H_0(x', y')$ provides a reference at zero voltage and the first exposure with respect to which the variation of the phase profiles can be obtained by applying increasing voltages and recording the corresponding holograms $H_i(x', y')$ (for i=1,...,269). Moreover, for each value of applied voltage several data are acquired to increase the precision of measurements. From the recorded holograms, the complex wave fields $O_i(x, y;L)=A_i(x, y)exp[i\Phi_i(x, y)]$ and $O_0(x, y; L)=A_o(x, y)exp[i\Phi_o(x, y)]$ (zero voltage reference object field) are numerically reconstructed at the same distance L=100 *mm* through Eq. (1). The phase difference $\Delta\Phi(x, y; L) = \Phi_i(x, y; L) - \Phi_0(x, y; L)$, wrapped in the range between –π and π, can be obtained by the following relation:

$$\Delta\Phi(x, y; L) = Arg\left\{\frac{\cos[\Phi_0(x, y)]\sin[\Phi_i(x, y)] - \cos[\Phi_i(x, y)]\sin[\Phi_0(x, y)]}{\cos[\Phi_0(x, y)]\cos[\Phi_i(x, y)] + \sin[\Phi_i(x, y)]\sin[\Phi_0(x, y)]}\right\}. \tag{3}$$

4. Spatially resolved refractive index profiles of CGH gratings: experimental results

The CGH-grating consists of a alternating sequence of polymer-rich stripes and liquid crystal-rich stripes in which the modulation of relative concentration of the two components and the refractive index mismatch between them gives rise to a H-PDLC-like grating. The polymer has a refractive index n_p=1.530, the extraordinary and ordinary refractive indices of the liquid crystal are n_e=1.799 and n_o=1.527, respectively (birefringence value $\Delta n=n_e- n_o\approx0.27$). By applying the external electric field, the refractive index of polymeric regions does not change significantly, because the liquid crystal (LC) concentration is negligible. The variation of grating fringe visibility measured by a polarized microscope, shows a preferential alignment of the droplet directors along the grating vector (*x*-axis in Fig. 2), i.e. along the direction orthogonal to the fringes. Consequently, it is expected that, with increasing voltage, the average reorientation of the LC droplets along the electric field direction causes a decrease of the average refractive index experienced by the light passing through the sample in correspondence of the liquid crystal fringes from a value ~n_e to ~n_o.

Let us define the average index profile $\left\langle n(x, y)\right\rangle_{\Delta V=0} = n_{on}(x, y)$, integrated along the sample thickness, at zero voltage ΔV=0 (the ON state of the grating). We also define $\left\langle n(x, y)\right\rangle_{\Delta V=V_{\max}} = n_{off}(x, y)$, the average index profile of the OFF state of the grating at maximum applied voltage, corresponding to the saturation level, $\Delta V=V_{max}$. Phase variations as a function of the external field can be conveniently referred to the zero voltage (ON state) in

#115297 - $15.00 USD Received 4 Aug 2009; revised 24 Sep 2009; accepted 28 Sep 2009; published 2 Oct 2009

order to optimize the reference and reduce the noise due to the temporal phase fluctuations. The reconstructed spatial distribution of the phase difference (absolute values)

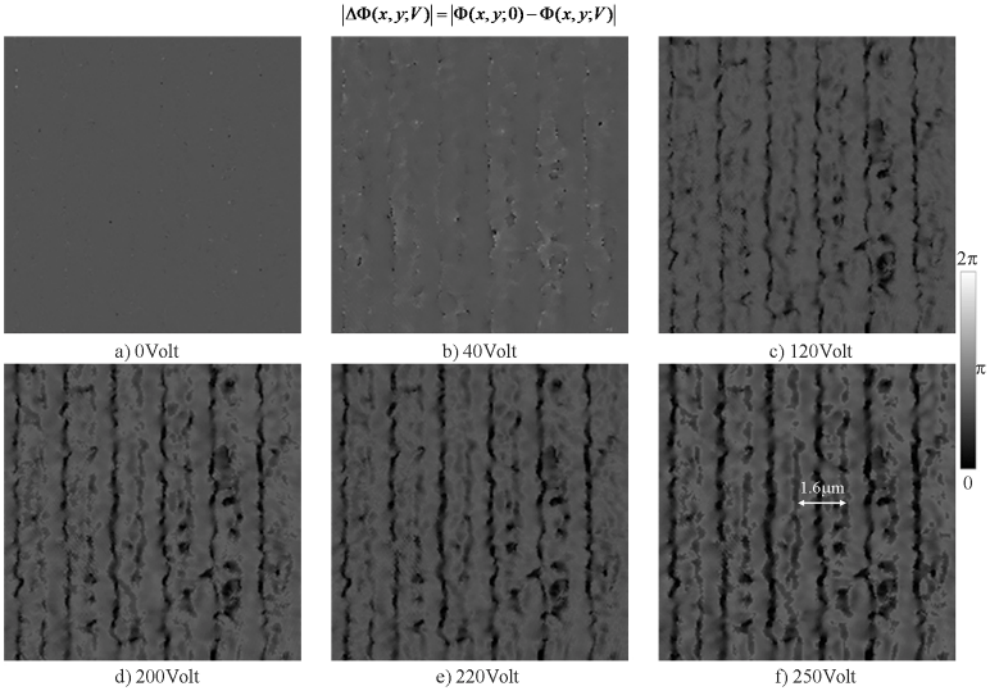

Fig. 3. Detail of phase difference profiles(absolute values) for a CGH-grating measured for increasing values of the external applied voltage.

are shown in Fig. 3: from Fig. 3-(a) to 3-(f), the phase profiles correspond to increasing values of the external applied voltage. The spatially resolved phase difference as a function of the applied voltage is defined by

$$|\Delta\Phi(x,y;V)| = |\Phi(x,y;0) - \Phi(x,y;V)| = \frac{2\pi}{\lambda} d \left| n_{on}(x,y) - \langle n(x,y) \rangle_V \right|, \qquad (4)$$

where $\langle n(x,y) \rangle_V$ indicates the average refractive index profile of the sample at generic electric potential difference $\Delta V=V$, integrated along the cell thickness d. For small values of the potential difference, the phase difference can be expanded up to the first order in ΔV

$$|\Delta\Phi(x,y;V)| = \frac{2\pi}{\lambda} d \left(\left| \frac{\partial \langle n(x,y) \rangle_V}{\partial V} \right|_{\Delta V=0} \right) \Delta V. \qquad (5)$$

It is worth pointing out that, in the ideal case of a uniform orientation of the LC molecular director along the grating vector, when the state is ON, we can have $n_{on}(x,y) \simeq n_e$ and in the OFF state, $n_{off}(x,y) \simeq n_o$. The actual modulation of the CGH-grating phase as a function of the magnitude of the applied electric field can be studied by determining the refractive index variation $\Delta\bar{n}$ between LC and polymer fringes. In Fig. 4-(a), the calculated refractive index variation $\Delta\bar{n}$ is plotted as a function of the external field magnitude for both *s*- and *p*-polarization of the incident light. The plotted data are obtained by taking the mean value of the refractive index difference along the grating profile. For *s*-polarization $\Delta\bar{n}$ can be can be well approximated by a linear fit with parameters $a=(3.42\pm0.015)\times10^{-3}$, $b=(-3.24\pm0.02)\times10^{-4}$

#115297 - $15.00 USD Received 4 Aug 2009; revised 24 Sep 2009; accepted 28 Sep 2009; published 2 Oct 2009

$\mu m/V$. For *p*-polarization of the incident light, we need to expand the phase difference up to second order ΔV in order to obtain a better agreement between the experimental data and the quadratic fitting curve with parameters $a=(6.65\pm0.04)\times10^{-3}$, $b=(-3.83\pm0.15)\times10^{-4}\mu m/V$, $c=(-2.3\pm0.1)\times10^{-5}\mu m^2/V^2$

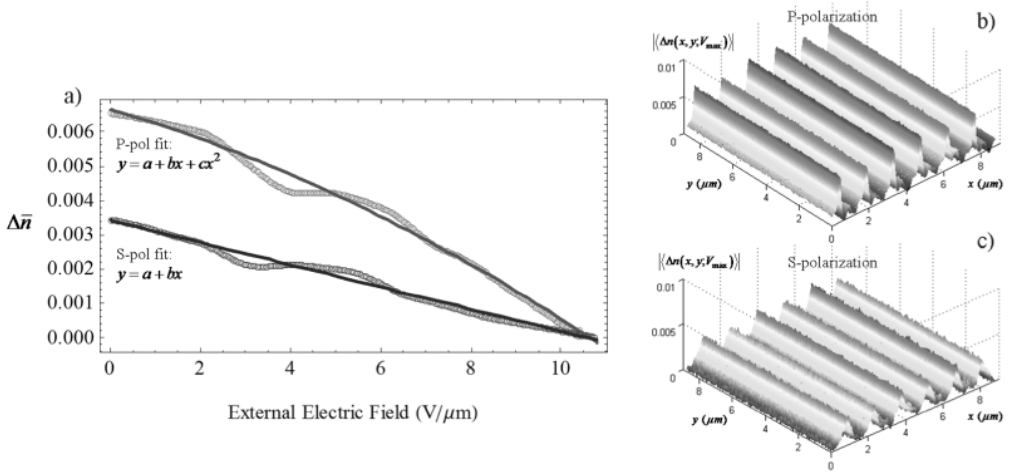

Fig. 4. (a) Mean value of the refractive index difference $\Delta\bar{n}$ as a function of the magnitude of the external electric field: agreement of experimental data measured on a CGH-grating for incident P-and S-polarization with quadratic and linear fitting lines, respectively. (b)-(c) Details of the spatially resolved refractive index profiles at the saturation voltage for (b) *p*-polarization and (c) *s*-polarization.

However, both the experimental curves show deviations with respect to the simple linear or quadratic fitting curves, for values of the electric field of about 3-4$V/\mu m$ and 5-6$V/\mu m$. These discrepancies are probably due to a threshold reorientation of the LC-droplets into the grating. Figure 4-(b) and 4-(c) show a detail of the spatially resolved average refractive index difference between the ON and OFF states of the grating for *p*- and *s*-polarization, respectively. The OFF state is reached at the saturation voltage $\Delta V=V_{max}$. The amplitude of the refractive index modulation is $\Delta n_{max}=(6.55\pm0.07)\times10^{-3}$ for *p*-polarization and $\Delta n_{max}=(3.45\pm0.07)\times10^{-3}$ for *s*-polarized light. These two values are in good agreement with the previously discussed behavior of the diffraction efficiency at the Bragg angle for the two polarizations (see Fig. 1-(a)). In fact, the diffraction efficiency is proportional to the optical contrast of the structure, to a good approximation. The ratio between the values of diffraction efficiencies for different polarization states shows that the amplitude of index modulation decreases by a factor of two in agreement with the experimental data of the refractive index modulation. Furthermore, the values of the optical contrast between the ON-OFF states agree with the parameters *a* estimating the refractive index difference between LC and polymer regions obtained from the fitting curves (in Fig. 4-(a)).

As previously discussed, the spatial resolution of the reconstructed phase profile is diffraction limited. For a probing wavelength $\lambda=532nm$, it is as of the order of 0.5-0.7μm. This means that for diffraction gratings with a pitch of the order 1-2μm, the interferometric technique is not capable of determining the morphology of the structure with sub-micron accuracy. Consequently, the phase modulation recorded for such kind of gratings can be regarded only as a spatially averaged measurement of the actual phase profile. However, for structures with larger grating spacing the technique allows to accurately determine the spatial morphology of the material. To this purpose, two examples of the spatially resolved refractive index profiles obtained in the case of CGH-grating with a pitch $\Lambda\simeq5\mu m$ for both *p*- and *s*-polarization are shown in Fig. 5-(a) and 5-(b), respectively. The mean amplitude of the refractive index modulation is $\Delta n_{max}=(7.88\pm0.14)\times10^{-3}$ for *p*-polarization and

#115297 - $15.00 USD Received 4 Aug 2009; revised 24 Sep 2009; accepted 28 Sep 2009; published 2 Oct 2009

$\Delta n_{max}=(4.50\pm0.08)\times10^{-3}$ for *s*-polarized light. As it can be clearly seen from the three-dimensional reconstruction of the index profile, the presence of liquid crystals droplets or domains embedded into the polymeric matrix gives rise to noisy index profile characterized by the presence of peaks with different size scale.

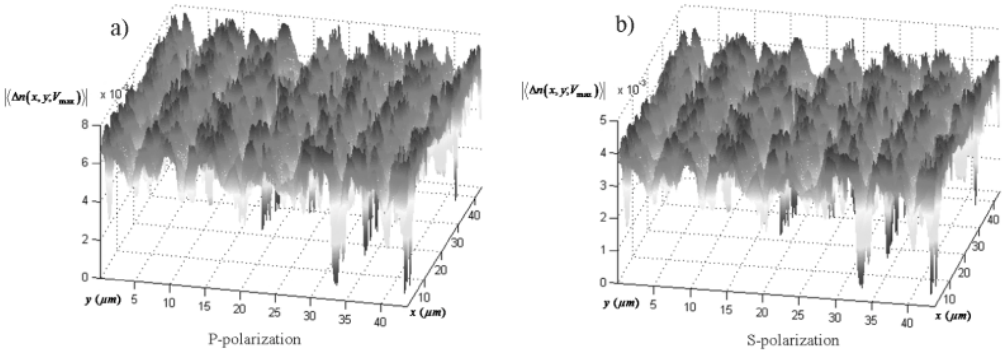

Fig. 5. Details of the spatially resolved refractive index profiles beam of a CGH-grating with grating pitch $\Lambda=5\mu m$ measured at the saturation voltage for (a) *p*-polarization and (b) *s*-polarization of the incident.

4. Conclusions

In this paper we have investigated on the polarization and switching properties of holographic gratings optically written into polymer/liquid crystal composites through single-beam spatial light modulation by means of computer-generated holograms. Measurements of the diffraction efficiency have shown a sensitive dependence of the electro-optic response of the CGH grating on the light polarization that indicated liquid crystal director ordering preferentially in the CGH-grating plane. A spatially resolved interferometric technique combined with a phase reconstruction method has been employed for measuring the two-dimensional spatial distribution of the refractive index change between the ON-OFF states of electrically switchable diffraction CGH gratings. The spatially resolved optical path difference was measured while a linearly rising voltage ramp was applied to the CGH grating. In particular, this technique has allowed to perform a morphological characterization of CGH-grating revealing a polymer-dispersed liquid crystal structure with liquid crystal droplets that appear to be oriented along the direction orthogonal to the grating fringes.

#115297 - $15.00 USD Received 4 Aug 2009; revised 24 Sep 2009; accepted 28 Sep 2009; published 2 Oct 2009